doi:10.1016/j.jmb.2011.08.049 J. Mol. Biol. (2011) 413, 699–711

Contents lists available at www.sciencedirect.com

Journal of Molecular Biology

journal homepage: http://ees.elsevier.com.jmb

Crystal Structure of Cardiac Troponin C Regulatory Domain in Complex with Cadmium and Deoxycholic Acid Reveals Novel Conformation

Alison Yueh Li[1,2]†, Jaeyong Lee[1]†, Dominika Borek[3], Zbyszek Otwinowski[3], Glen F. Tibbits[1,2,4] and Mark Paetzel[1,2]*

[1]*Department of Molecular Biology and Biochemistry, Simon Fraser University, South Science Building, 8888 University Drive, Burnaby, British Columbia, Canada V5A 1S6*
[2]*Department of Biomedical Physiology and Kinesiology, Molecular Cardiac Physiology Group, Simon Fraser University, 8888 University Drive, Burnaby, British Columbia, Canada V5A 1S6*
[3]*Department of Biochemistry, University of Texas Southwestern Medical Center at Dallas, 5323 Harry Hines Boulevard, Dallas, TX 75390, USA*
[4]*Cardiovascular Sciences, Child and Family Research Institute, 950 West 28th Avenue, Vancouver, BC, Canada V5Z 4H4*

Received 20 June 2011; received in revised form 23 August 2011; accepted 24 August 2011
Available online 6 September 2011

Edited by R. Huber

Keywords:
troponin C;
EF-hand;
cadmium ion coordination;
deoxycholic acid;
radiation damage

The amino-terminal regulatory domain of cardiac troponin C (cNTnC) plays an important role as the calcium sensor for the troponin complex. Calcium binding to cNTnC results in conformational changes that trigger a cascade of events that lead to cardiac muscle contraction. The cardiac N-terminal domain of TnC consists of two EF-hand calcium binding motifs, one of which is dysfunctional in binding calcium. Nevertheless, the defunct EF-hand still maintains a role in cNTnC function. For its structural analysis by X-ray crystallography, human cNTnC with the wild-type primary sequence was crystallized under a novel crystallization condition. The crystal structure was solved by the single-wavelength anomalous dispersion method and refined to 2.2 Å resolution. The structure displays several novel features. Firstly, both EF-hand motifs coordinate cadmium ions derived from the crystallization milieu. Secondly, the ion coordination in the defunct EF-hand motif accompanies unusual changes in the protein conformation. Thirdly, deoxycholic acid, also derived from the crystallization milieu, is bound in the central hydrophobic cavity. This is reminiscent of the interactions observed for cardiac calcium sensitizer drugs that bind to the same core region and maintain the "open" conformational state of calcium-bound cNTnC. The cadmium ion coordination in the defunct EF-hand indicates that this vestigial calcium binding site retains the structural and functional elements that allow it to coordinate a cadmium ion. However, it is a result of, or concomitant with, large and unusual structural changes in cNTnC.

*Corresponding author. Department of Molecular Biology and Biochemistry, Simon Fraser University, South Science Building, 8888 University Drive, Burnaby, British Columbia, Canada V5A 1S6. E-mail address: mpaetzel@sfu.ca.

† A.Y.L. and J.L. contributed equally to this work.

Abbreviations used: cTnC, cardiac troponin C; cNTnC, amino-terminal domain of cTnC; DXC, deoxycholic acid; EF 1, EF-hand motif 1; EF 2, EF-hand motif 2; ASU, asymmetric unit; TnC, troponin C; sTnC, skeletal troponin C; PDB, Protein Data Bank; SAD, single-wavelength anomalous dispersion; Se-Met, selenomethionine; NTnC, N-terminal domain of TnC.

Introduction

Troponin C (TnC) is a regulatory Ca^{2+} binding subunit in the troponin complex that mediates muscle contraction. The troponin complex, which consists of TnC, TnI, and TnT subunits, is located periodically on the thin filaments composed of tropomyosin and actin monomers.[1] During muscle contraction, Ca^{2+} binding to the N-terminal domain of TnC (NTnC) initiates a conformational change that exposes its central hydrophobic cavity. A change in the binding interactions by the inhibitory subunit TnI, from the actin monomers to the TnC hydrophobic core, triggers an overall conformational change within the troponin complex. The final outcome is the cross-bridge cycle that results in muscle contraction.[2] NTnC therefore plays the crucial role of a cytosolic Ca^{2+} sensor in skeletal and cardiac muscle function.

NTnC consists of two EF-hand motifs [EF-hand motif 1 (EF 1) and EF-hand motif 2 (EF 2)], which are commonly present in Ca^{2+} binding proteins (Fig. 1a). The classical EF-hand motif consists of two α-helices oriented approximately perpendicularly to one another and linked by a loop that is normally 12 residues long.[3] The residues at loop positions 1, 3, 5, 7, and 12 are normally involved in the ion coordination[4] (Fig. 1). Canonically, a Ca^{2+} is coordinated by seven oxygen atoms in pentagonal bipyramidal geometry. The five equatorial plane ligands from single carbonyl groups at Y, Z, and −Y and a bidentate ligand from a glutamate side-chain carboxylate at the −Z positions are complemented by two single axial ligands at the X and −X positions.

Two muscle-specific TnC proteins are expressed in vertebrate muscles. Skeletal troponin C (sTnC) in fast skeletal muscle and cardiac troponin C (cTnC) in cardiac and slow skeletal muscle differ mostly in the primary sequence and Ca^{2+} binding property of the EF 1 ion binding loop of NTnC (Fig. 1b). In the mammalian amino-terminal domain of cTnC (cNTnC), the loop sequence deviates from the canonical sequence by insertion of Val28, resulting in the extension of the loop to 13 residues and substitutions of the two normally chelating aspartate residues by the nonpolar Leu29 and Ala31 residues.[5] This results in loss of Ca^{2+} binding function by the loop.[6,7] The functional EF 2 with canonical loop sequence and a relatively low Ca^{2+} binding affinity ($\sim 10^5\ M^{-1}$)[8] is then proposed to act alone as the cytosolic Ca^{2+} sensor for the cardiac troponin complex.[6]

Nevertheless, nuclear magnetic resonance (NMR) studies indicate that there is a structural and dynamic coupling between the two EF-hands that may play a functional role.[9] Other evidence also suggests that EF 1 has a role in the function of cNTnC. For example, ectothermic species of vertebrates adapted to colder climates have a

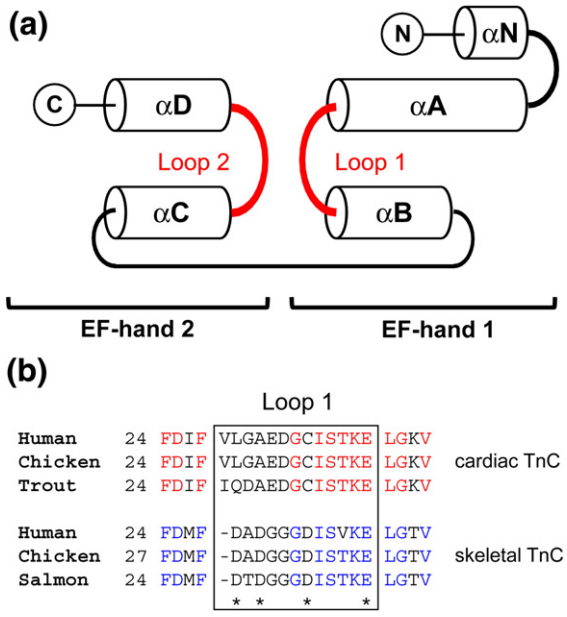

Fig. 1. The topology of NTnC and the sequence variability observed within loop 1. (a) NTnC is composed of five α-helices that are labeled N, A, B, C, and D. The five α-helices assemble into two helix–loop–helix motifs (EF-hand motifs). EF-hand 1 is composed of helices αA and αB and loop 1 (red); EF-hand 2 is composed of αC and αD and loop 2 (red). (b) A sequence alignment of ion binding loop 1 (boxed) and surrounding residues in the first EF-hand motif of NTnC. The cardiac NTnC sequences shown are those from human (Swiss-Prot accession number: P63316), chicken (P09860), and trout cNTnC (Q7ZZB9). The skeletal NTnC sequences are those of human (P02585), chicken (P02588), and Atlantic salmon (B9EP57). The residues conserved throughout are colored red for cTnC and blue for sTnC. The skeletal NTnC loop 1 residues that coordinate Ca^{2+} are indicated by stars.

significantly different sequence in the N-terminal portion of the EF 1 loop (Fig. 1b). In trout, the substituted residues Ile28, Gln29, and Asp30 appear to be responsible for increasing Ca^{2+} affinity which enables trout cardiac function at significantly lower temperatures.[10] Interestingly, these substitutions are not observed in certain semitropical ectotherms (e.g., *Anolis carolinensis* or green anole-accession number GI 327265790) that thrive at 25–30 °C and exhibit complete identity with human cTnC over the first 60 amino acids. Clearly, these substitutions are related to functionality at a given temperature as was postulated.[10,11] Intriguingly, one of the characteristic substitutions found in the trout and other teleosts (L29Q) has been observed as a mutation in a patient diagnosed with an inherited cardiac muscle disorder known as familial hypertrophic cardiomyopathy.[12]

Derived from ongoing structural studies, 12 cNTnC structures solved by NMR spectroscopy and 5 by X-ray crystallography are currently

available in the Protein Data Bank (PDB) (Supplementary Table 1). Most of these structures represent the cNTnC domain (residues 1–89) in a Ca^{2+}-saturated form with Ca^{2+} coordination shown only by EF 2, while no ion coordination is observed in the dysfunctional binding site of EF 1. However, all crystal structures of cNTnC are that of a mutant version with two substitution mutations (C35S and C84S) introduced to prevent potential intermolecular and intramolecular disulfide bond formation.[13] Although the mutant cTnC was shown to have the same functional properties as the wild type *in vitro*,[13,14] Cys35 is a part of the EF 1 loop and highly conserved phylogenetically in cNTnC (Fig. 1b).[11]

To address the lack of crystallographically determined structures of the wild-type cNTnC domain, we have over-expressed, purified, and successfully crystallized the human cNTnC domain with the wild-type primary sequence. This was achieved under a novel crystallization condition that contained cadmium sulfate and deoxycholic acid (DXC). The crystal structure was then solved using single-wavelength anomalous dispersion (SAD) methods and refined to 2.2 Å resolution. Surprisingly, the structure revealed cNTnC in a highly unique conformation, which permits both EF-hand motifs to coordinate cadmium (Cd^{2+}) ions in a canonical bipyramidal pentagonal geometry. This unique conformation is also stabilized in part by DXC bound to the central hydrophobic core cavity. Analysis of the novel ion coordination state by EF 1 demonstrates that the vestigial loop retains structural and functional elements that enable cadmium ion binding. These elements are reminiscent of the versatile noncanonical EF-hand motifs;[15,16] however, this coordination is achieved as a result of or concomitant with large and unusual structural changes in cNTnC.

Results and Discussion

Structure solution: Dealing with radiation damage and pseudosymmetry

The novel crystals of human cNTnC (residues 1–89) with wild-type primary sequence diffracted to 2.2 Å resolution. However, finding a structure solution via anomalous diffraction techniques or molecular replacement methods presented serious challenges due to the presence of translational pseudosymmetry and the heavy dose of X-ray radiation absorbed in the crystal during data collection. The physical deterioration of the crystal during exposure to the X-ray beam caused not only a gradual decay of diffraction intensities and structure factor amplitudes but also structural rearrangements in the crystal lattice, hindering phasing procedures and subsequent refinements.[17,18] The presence of 50 mM Cd^{2+} in the crystallization solution contributed to an increased X-ray absorption without improving the scattering power of the crystal, resulting in an increased rate of radiation damage and additional diffused background. Moreover, the presence of ordered cadmium ions increased the number of heavy-atom sites that needed to be identified by direct methods. The number of selenomethionine (Se-Met) and cadmium positions was relatively high due to the presence of four molecules in the asymmetric unit (ASU). Without pseudotranslational symmetry, these problems could still be solved without much trouble. However, the crystallographic direct methods in their design assume random positions of heavy atoms and are severely handicapped by the presence of pseudotranslational symmetry, which generates a highly nonrandom pattern of inter-atom distances. The combination of radiation-induced changes, high number of heavy-atom scatterers to be found, and translational pseudosymmetry (native Patterson peak height of 47.8% of origin at 0.5, 0.5, 0.5) resulted in a borderline solvable phasing problem. The Se-Met crystal structure was solved by the SAD method from a data set collected at the selenium peak wavelength (Se-Met data 1). The structure was then refined to 2.2 Å resolution using the second anomalous data set that did not initially yield a SAD solution (Se-Met data 2). Merging statistics for Se-Met data set 1 used for experimental phasing and Se-Met data set 2 used for final refinement are shown in Table 1.

The protein crystal has unit cell dimensions of 51.9 Å × 81.9 Å × 100.5 Å and belongs to the orthorhombic space group $P2_12_12$. The ASU contains four protein chains with 53.5% solvent content and has a Matthews coefficient of 2.7 $Å^3\ Da^{-1}$. The four chains are denoted as chain A (Asp3–Met85), chain B (Tyr5–Val82), chain C (Asp3–Met85), and chain D (Tyr5–Val82). Missing residues at the N- and C-termini could not be modeled due to a lack of clear electron density. Chains A and B form a dimer with a 2-fold non-crystallographic symmetry and are related to another dimer consisting of chains C and D by a translation with a (0.5, 0.5, 0.5) vector exhibiting a translational pseudosymmetry. A total of 21 cadmium ions, 3 calcium ions, and 5 DXC molecules were modeled with the protein chains. The final refined structure has an *R*-factor of 22.5% and an R_{free} of 28.1%. The average *B*-factor of the structure is 41.3 $Å^2$ (Table 1).

An unusual cNTnC conformation stabilized by cadmium binding

The overall conformation of cNTnC revealed in the crystal structure is a pair of EF-hand motifs connected by a linker sequence (Fig. 2a). The first EF-hand motif (EF 1), which follows a short α-helix N (residues 4–10), consists of α-helix A

Table 1. Data collection, phasing, and refinement statistics

Crystal parameters	Se-Met data 1[a]	Se-Met data 2
Space group	$P2_12_12$	$P2_12_12$
a, *b*, *c* (Å)	51.8, 81.8, 100.5	51.8, 81.8, 100.5
Data collection statistics		
Wavelength	0.98068	0.98066
Resolution (Å)	2.5–50.0 (2.5–2.6)[b]	2.2–50.0 (2.2–2.3)
Total reflection	75,935	85,499
Unique reflection	14,864 (1414)	22,061 (2192)
R_{merge}[c]	0.081 (0.091)	0.067 (0.176)
Mean $(I)/\sigma(I)$	26.2 (4.1)	28.4 (5.7)
Completeness	95.5 (93.8)	98.4 (99.1)
Redundancy	4.0 (3.4)	3.9 (3.8)
Phasing statistics		
Overall figure of merit	0.23	
Refinement statistics		
Protein molecules in asymmetric unit		4
Residues		322
Water molecule		133
Total number of atoms		2815
Number of deoxycholate ions		5
Number of cadmium ions		21
Number of calcium ions		3
R_{cryst}[d]/R_{free}[e](%)		22.5/28.1
Average *B*-factor (Å^2)		41.3
r.m.s.d. on angles (°)		1.89
r.m.s.d. on bonds (Å)		0.03
Ramachandran analysis (%)		
Preferred regions		271 (96.1)
Allowed regions		11 (3.9)
Outliers		0 (0.00)
B-factor		
Overall		41.3
cNTnC chain A		35.2
cNTnC chain B		37.8
cNTnC chain C		47.1
cNTnC chain D		44.1
Deoxycholate ions		58.5
Cadmium ions		39.3
Calcium ions		57.6
Water molecules		27.5
Residues missing from the models due to a lack of electron density		
Chain A		1–2, 86–89
Chain B		1–4, 83–89
Chain C		1–2, 86–89
Chain D		1–4, 83–89

[a] Se-Met data 1 was used to obtain initial phase estimates, and Se-Met data 2 was used for structure refinement.

[b] The data collection statistics in brackets are the values for the highest-resolution shell.

[c] $R_{merge} = \sum_{hkl}\sum_i |I_i(hkl) - \langle I(hkl)\rangle| / \sum_{hkl}\sum_i I_i(hkl)$, where $I_i(hkl)$ is the intensity of an individual reflection and $\langle I(hkl)\rangle$ is the mean intensity of that reflection.

[d] $R_{cryst} = \sum_{hkl} ||F_o| - |F_c|| / \sum_{hkl} |F_o|$, where F_o and F_c are the observed and calculated structure factor amplitudes, respectively.

[e] R_{free} is calculated using 5% of the reflections randomly excluded from refinement.

(residues 14–31), ion binding loop 1, and α-helix B (residues 38–47). The second EF-hand motif (EF 2) consists of α-helix C (residues 54–64), ion binding loop 2, and α-helix D (residues 74–84). The two EF-hand motifs are connected by a linker that spans residues 48–53. All four protein chains in the ASU have similar conformations. The backbone superimposition of the four chains results in a root-mean-square deviation (r.m.s.d.) of 0.73 Å. The major discrepancies between the chains occur at the terminal helices and the linker region that connects helix B and helix C.

In comparison to a previously solved crystal structure of human cNTnC in a Ca^{2+}-saturated form (PDB ID: 1WRK), the structure presented here adopts a very different conformation with dramatic changes at helix A (Fig. 2b and c). Similar changes are also observed in comparison with various NMR structures (Supplementary Fig. 1). Firstly, residues Val28–Ala31, normally part of a disordered and dysfunctional loop, adopt an α-helical conformation, resulting in an extension of helix A at its C-terminal end (Fig. 2d). Secondly, unlike the classical EF-hand motif in which the two helices are oriented almost perpendicularly, helix A is oriented antiparallel with helix B (Fig. 2c). This conformation is stabilized in part by van der Waals interactions between the helices. This also obliterates the 2-fold rotational symmetry between the pair of EF-hand motifs, which is a common feature in NTnC structures. Finally, loop 1 in EF 1, previously considered to be dysfunctional, is coordinating a Cd^{2+}.

The electron densities that clearly indicated metal ions being coordinated by both EF 1 and EF 2 were fitted with Cd^{2+} for the following reasons. First, cadmium ions were identified on the anomalous difference map. There were three potential anomalous scatterers in the crystal: selenium from Se-Met, calcium from the protein purification solution, and cadmium from the crystallization condition. Se-Met positions were clearly defined by Se-Met residues. There were 21 other peaks outside of the anomalous peaks describing Se-Met positions. At the data collection wavelength, the cadmium anomalous signal is 3.4 times larger than the signal arising from calcium. The observed signal was thus only consistent with cadmium as it was too strong to originate from calcium ions. Second, Cd^{2+} has an ionic radius of 0.97 Å, which is very close to that of Ca^{2+} (0.99 Å) and can be coordinated by TnC without causing much perturbation in its overall conformation.[19,20] Third, in the binding loop of EF 1, one of the coordinating ligands is sulfur from Cys35. Other examples of Cd^{2+} coordination frequently involve a cysteine residue.[21] Finally, the refinement statistics agree with cadmium ions being present at these sites (Table 1).

Cadmium ions are also found outside the ion binding loops. An extra Cd^{2+} is present in close proximity of every Cd^{2+} coordinating loop, with residues from the loop contributing to its interaction. Cadmium ions are also found between protein chain interfaces and they contribute to the interchain crystal packing contacts. For

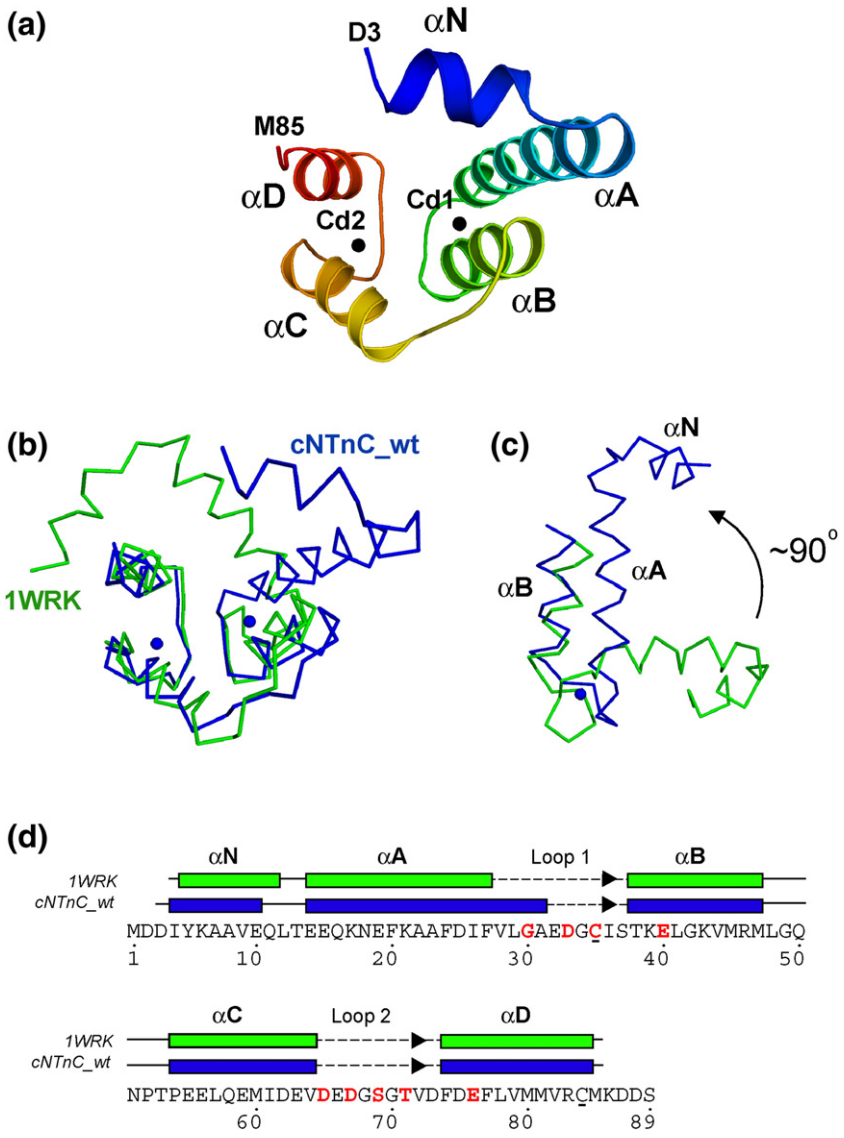

Fig. 2. The protein fold of human cNTnC with structural comparisons. (a) A cartoon rendering of human cNTnC (chain A) is colored spectrally from the N-terminus (blue) to the C-terminus (red). The amino- and carboxyl-termini and five helices N, A, B, C, and D are labeled. The cadmium ions coordinated by the ion binding loops are shown as black spheres (Cd1 and Cd2 are Cd101 and Cd102 in PDB: 3RV5 respectively). (b) Chain A of human wild-type cNTnC (blue) is superimposed with human cNTnC (C35S and C84S mutant) complexed with trifluoperazine (PDB ID: 1WRK) (green). The bound cadmium ions are shown as blue spheres. (c). The comparison of the first EF-hand motif in the superimposed structures. The major structural difference is the relative position of helix N and helix A with respect to helix B. There is a ~90° shift in this region of the structure when compared to 1WRK. (d). The secondary structure elements of this human cNTnC chain A (blue) and 1WRK are overlaid with the sequence of human cNTnC. The arrows indicate the main-chain hydrogen bond formed between Ile36 and Val72. The residues that coordinate Cd^{2+} in this structure are colored red. The Cys35 and Cys84 residues mutated to serine in 1WRK are underlined.

example, one Cd^{2+} is coordinated by both Cys35 of chain A and the carboxylate side chains of Glu15 and Glu19 from its symmetry-related counterpart, while another Cd^{2+} is coordinated by Glu32 of chain B and Glu15 of chain C. A total of 21 cadmium ions are found near the binding loops and the protein chain interfaces. Their complex coordination networks stabilize the unusual conformation of cNTnC and maintain the critical protein contacts within the protein crystal.

Cadmium coordination by EF 1 and EF 2

All four cNTnC protein chains in the ASU coordinate a Cd^{2+} in the binding loop of EF 1. In three chains (chains A, B, and D), Cd^{2+} coordination adopts the canonical seven-ligand pentagonal bipyramidal geometry (Fig. 3a). The remaining chain C coordinates Cd^{2+} in a six-ligand octahedral geometry for reasons discussed below. Only four residues, Gly30, Asp33, Cys35, and Glu40, supply the coordinating ligands. The five equatorial plane ligands are Asp33 $O^{\delta 1}$ (Y) and $O^{\delta 2}$ (Z), Cys35 O (−Y), and Glu40 $O^{\varepsilon 1}$ and $O^{\varepsilon 2}$ (−Z). These are complemented by two axial ligands, Gly30 O (X) and Cys35 S (−X) (Table 2).

The Cd^{2+} coordination state in the ion binding loop of EF 2 is identical in all four cNTnC molecules of the ASU. It adopts the canonical seven-ligand pentagonal bipyramidal coordination with ligands from five conserved residues: Asp65 (X), Asp67 (Y), Ser69 (Z), Thr71 (−Y), and Glu76 (−Z) and one water molecule (−X) (Fig. 3b). The coordinating ligands are listed in Table 2. The ligands and backbone conformation of the loop are virtually identical with the Ca^{2+} coordination by EF 2 in other cTnC structures. The backbone of the coordinating loop region (Asp65–Glu76) aligns with r.m.s.d. values of

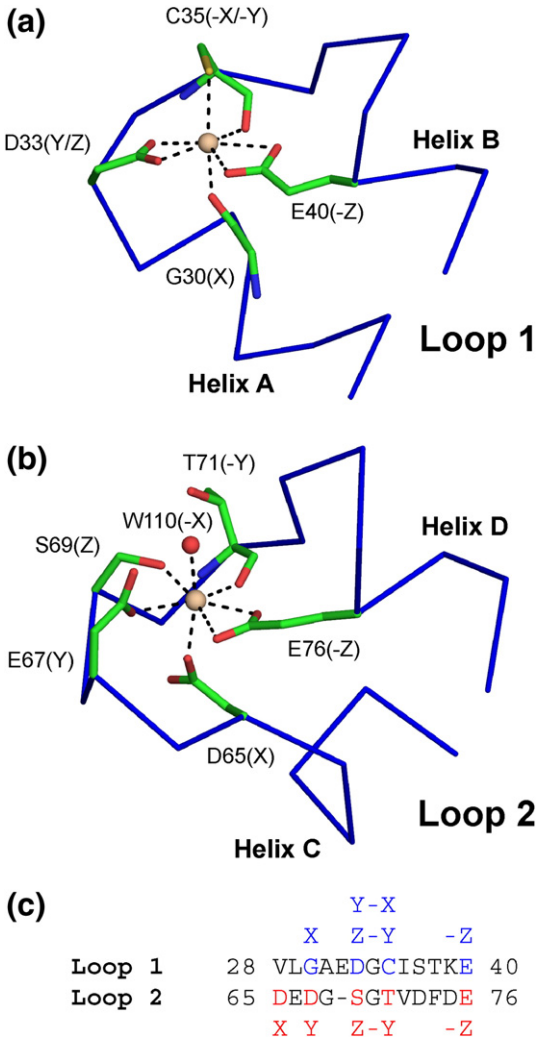

Fig. 3. The coordination of cadmium ions in human cNTnC. The residue side chains that are directly involved in the Cd^{2+} coordination are shown in stick (carbon, green; oxygen, red). The protein main chain is shown as blue C^{α} trace. The water molecule is shown as a red sphere, and the cadmium ions are shown as larger wheat-colored spheres. (a) Cd^{2+} coordination in pentagonal bipyramidal geometry in the noncanonical loop 1 of EF 1. (b) A canonical Cd^{2+} coordination in loop 2 of EF 2. (c) The amino acid sequences for EF 1 loop 1 (residues 28–40) and EF 2 loop 2 (residues 65–76) are aligned, and the residues involved in ion coordination are colored blue (loop 1) and red (loop 2). The ligand coordination positions for the participating residues are indicated in the same color.

0.4 Å with 1J1E[22] 0.3 Å with 1WRK (Takeda, S., Igarashi, T., Oishi, Y., and Mori, H., unpublished data). The similarity of calcium and cadmium coordination has previously been corroborated by other calcium binding proteins such as calbindin D9k, which displays comparable coordination of Cd^{2+} in solution to that of Ca^{2+}.[23]

Table 2. Canonical cadmium ion coordination by loop 1 and loop 2 in wild-type cNTnC chain A

	Loop 1			Loop 2		
Position	Residue	Atom	Distance (Å)	Residue	Atom	Distance (Å)
	Val28					
	Leu29					
X	Gly30	O	2.2	Asp65	$O^{\delta 2}$	2.1
	Ala31			Glu66		
	Glu32					
Y	Asp33	$O^{\delta 1}$	2.4	Asp67	$O^{\delta 1}$	2.3
				Gly68		
Z	Asp33	$O^{\delta 2}$	2.1	Ser69	O^{γ}	2.3
	Gly34			Gly70		
−Y	Cys35	O	2.5	Thr71	O	2.4
−X	Cys35	S	2.5	W110	O	2.3
	Ile36			Val72		
	Ser37			Asp73		
	Thr38			Phe74		
	Lys39			Asp75		
−Z	Glu40	$O^{\varepsilon 1}$	2.4	Glu76	$O^{\varepsilon 1}$	2.3
		$O^{\varepsilon 2}$	2.6		$O^{\varepsilon 2}$	2.6

Comparison of the loop sequences (Fig. 3c) shows that the absence of two chelating glutamate residues in the N-terminal part of loop 1 does not permit ion coordination in the same canonical conformation as in loop 2. Instead, loop 1 has compensated for the difference in adopting a novel backbone fold and coordination characteristics to fulfill the canonical geometry.

The first novel characteristic is that the carboxylate group of Asp33 is in a planar orientation to the equatorial plane of the Cd^{2+} and ligand interactions. Canonically, an aspartate residue in the equivalent position contributes only one oxygen atom from its carboxylate group and occupies a single Z position. However, in the structure presented here, the Asp33 bidentate ligand occupies both Y and Z coordination positions in chains A, B, and D. In chain C, Asp33 does not occupy both positions, and because of this, the Cd^{2+} coordination fails to adopt the canonical geometry. We are not aware of any other examples of one aspartate residue providing bidentate ligands for both Y and Z positions.

A second unique characteristic is the ion coordination shown by Cys35. Normally, the equivalent residue supplies the backbone carbonyl atom for only the −Y ligand position. In the structure presented here, as well as the backbone carbonyl, the sulfur side-chain atom of Cys35 is involved in ion coordination at the −X ligand position, which is normally occupied by a water molecule. We could not find another example of an EF-hand motif that utilizes cysteine as one of the coordinating ligands. The extra coordination may be due to the nature of the bound ion. Chemically, Cd^{2+} is a soft metal ion and would preferentially coordinate soft atoms such as sulfur.[24] However, Ca^{2+}, which is a hard metal ion, would not normally prefer sulfur as a ligand.

The final and the most striking characteristic is the coordination by the Gly30 carbonyl oxygen at position X. The N-terminal residues of ion binding loop 1, including Val28, Leu29, and Gly30, are involved in unique conformational changes. From the "disordered loop" conformation in the absence of ion binding, they adopt a helical conformation and become the C-terminal part of an extended helix A. These conformational changes, as well as a dramatic shift in the orientation of helix A, results in the positioning of Gly30 O into a proximity and orientation to the bound Cd^{2+} for direct coordination.

Comparison of cNTnC EF 1 with noncanonical EF-hands

Calcium binding EF-hand proteins show significant diversity in the loop length and sequence composition of the calcium binding loop.[15,16] Large differences are accommodated by adjustments within the backbone conformation such that the canonical coordination geometry is not changed. This frequently involves employing backbone carbonyl oxygens as the coordinating ligands. Like the cNTnC loop 1, the EF1 Ca^{2+} binding loop sequence of *Arabidopsis thaliana* calcineurin-B-like protein (AtCBL2) (PDB ID: 1UHN)[25] is markedly different from that of the classical EF-hand loop. The N-terminal part of the loop is extended by two residues and it lacks the highly conserved aspartate residues at X and Y positions.[25] It can nevertheless coordinate a Ca^{2+} in canonical pentagonal bipyramidal geometry. A unique main-chain conformation allows two main-chain backbone carbonyl oxygens to replace the canonical side-chain carboxylate oxygens for the X and Y ligand positions. Similar to the structure presented here, the main-chain carbonyl oxygen at the X position comes from a residue in the entering helix.

The canonical and noncanonical Ca^{2+} binding loops nevertheless share a highly conserved C-terminus.[15] Compared to the more dynamic N-terminal region, the C-terminal region is highly stabilized by the turn of the exiting helix and a hydrogen bond to the other ion binding loop of the paired EF-hand motif.[9] This highly conserved sequence and structural features exist in the Cd^{2+} coordinating loop 1 of the structure presented here. First, the ligand at the −Y position is the main-chain carbonyl oxygen (Cys35). This residue is then followed by a hydrophobic residue (Ile36), which is involved in β-sheet hydrogen bonding interaction with an equivalent residue (Val72) in the opposite loop (known as the "EF β-scaffold").[15] The ligand at the −Z position is a bidentate interaction from a glutamate residue sidechain carboxylate (Glu40), and there is a four-residue spacing between the −Y and −Z ligands. The structural alignment of the backbone atoms of these conserved C-terminal residues in the loops of EF 1 (Asp33–Glu40) and EF 2 (Ser69–Glu76) results in an r.m.s.d. of 1.2 Å.

The Cd^{2+} coordination by loop 1 lacks the extensive loop-stabilizing hydrogen bond interactions of the Ca^{2+} coordinating EF-hand motifs between the residues that comprise the loop. EF 1 contains relatively few residues participating in Cd^{2+} coordination, and the absence of chelating aspartate residues results in less extensive hydrogen bonding interactions as compared with EF 2. Moreover, the overall conformational change induced by the Cd^{2+} binding in loop 1 is uncharacteristic of NTnC. The Ca^{2+} binding in classical EF-motifs normally decreases the interhelical angle from ~135° to 90°. The Cd^{2+}-induced conformational change in EF 1 is the opposite, as the resulting interhelical angle increases to ~180° (~antiparallel helices). The rotation of helix A is approximately centered at Leu29. As a result, helix N and helix A have completely lost contact with helix D. The unusual antiparallel helical conformation adopted by the EF 1 appears similar to that of the non-Ca^{2+} binding EF-hand motif in the N-terminal EF-hand pair of recoverin.[26] However, the helices are antiparallel only in the Ca^{2+}-free state of the protein. The Ca^{2+} binding by the other functional EF-hand motifs results in a conformational change that rotates the entering helix outward with marked changes in the interhelical angle.[27] Thus, the conformational change observed in our structure is the opposite to that of recoverin and unique among available NTnC structures.

The binding of DXC in the "open" core

DXC, a by-product of intestinal bacteria, is a steroid acid commonly found in the bile of mammals (Fig. 4a).[28] DXC is used as a mild detergent for the isolation of membrane-associated proteins[29] and was used for the optimization of the cNTnC crystallization condition. The inclusion of DXC resulted in crystals with a different morphology and space group when compared to those grown without DXC. The electron density is consistent with two DXC molecules being associated with chain A (Fig. 4b). One DXC molecule (DXC1) is present in the central hydrophobic cavity that is formed by a cluster of several hydrophobic residues. These include the aromatic ring of Phe27 from helix A, the side chains of Leu41, Val44, SeMet45, and Leu48 from helix B, and the side chains of Phe77 and SeMet81 from helix D. The calculated total surface area of the pocket is approximately 503 $Å^2$. Electron density for DXC is present in all chains, but the density is clearest in chain A. The hydrophobic fused rings of DXC are bound within the hydrophobic cavity, while its carboxylate group is exposed to solvent. The other DXC molecule (DXC2) is bound to a

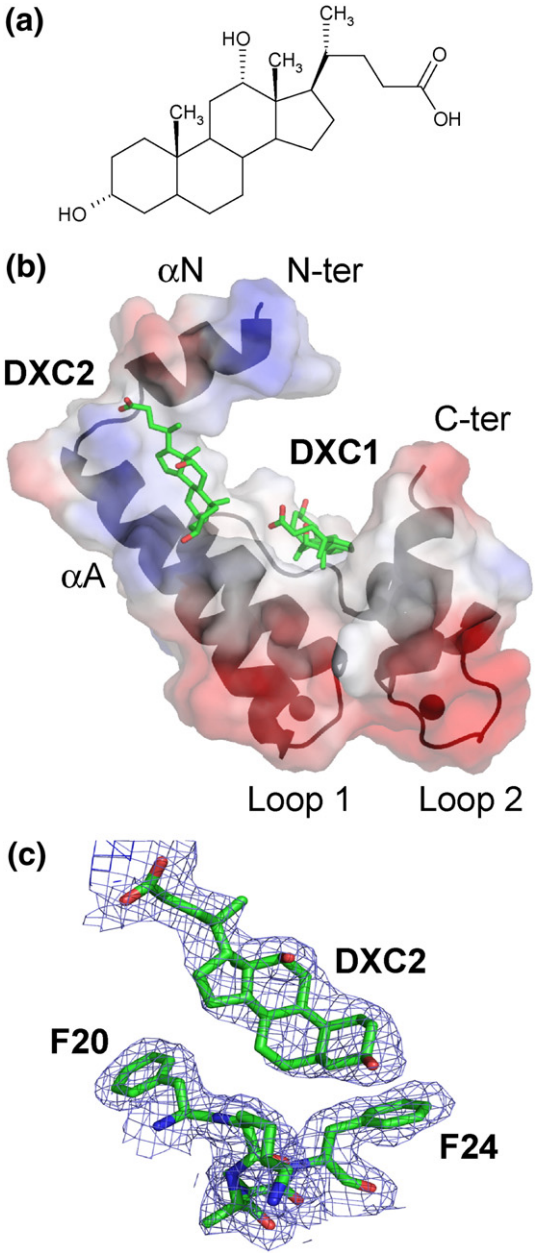

Fig. 4. DXC binding interactions with human cNTnC. (a) The chemical structure of DXC. (b) DXC binding sites on cNTnC. DXC is shown in stick format, and cNTnC (chain A) is rendered as semitransparent surface with mapped electrostatic surface. (White, neutral; blue, positive; red, negative). DXC1 (*DXC91* in PDB: 3RV5) is bound at the central hydrophobic cavity, while DXC2 (*DXC92* in PDB: 3RV5) is bound between αN and αA. (c) A sample of the $2F_o - F_c$ electron density map contoured at 1.0 σ is shown for residues Phe20 to Phe24 of chain A and the nearby DXC2.

hydrophobic patch on helix N and helix A. The details of its interaction differ in each chain. In chain A, the binding of the DXC2 molecule is stabilized by a ring stacking interaction with the aromatic ring of Phe24 and a hydrogen bonding interaction with the Lys17 N^{ζ} of chain A. The carboxylate group of DXC2 also coordinates a Cd^{2+} with Glu59 $O^{\varepsilon 1}$ and Glu59 $O^{\varepsilon 2}$ of chain B.

The DXC molecule has features similar to those of the Ca^{2+} sensitizing drugs such as trifluoroperzaine (Takeda, S., Igarashi, T., Oishi, Y., and Mori, H., unpublished data), EMD 57033,[30] and levosimendan.[31] They each have at least two hydrophobic fused rings and a hydrophilic head group. As listed below, structures in complex with these drugs show that the hydrophobic ring system binds to the hydrophobic pocket within TnC and the hydrophilic head group is often exposed to the solvent. The hydrophobicity and flexibility of the DXC appear to be an important feature for its interaction with cNTnC (Fig. 4c).

Structural comparison with other cNTnC structures

Several of the drugs known as the Ca^{2+} sensitizers are used to treat heart failure, which is a condition characterized by the inability of the heart to supply sufficient blood flow to vital organs.[32,33] The mechanisms utilized by these Ca^{2+} sensitizers vary widely, but in general, they tend to increase the Ca^{2+} affinity of the troponin complex to improve cardiac muscle contractility without directly increasing the cytosolic Ca^{2+} concentration, which could potentially result in arrhythmia and diastolic dysfunction.[33] Since the regulatory domain of cTnC serves an important role as a Ca^{2+} sensor, the structure of cNTnC in complex with a Ca^{2+} sensitizer molecule and the switch peptide of cTnI ($cTnI_{147–163}$) has been investigated extensively in recent years.[14,34–36] A number of the NMR and the crystal structures show that these Ca^{2+} sensitizers may function by binding to the hydrophobic cavity of cNTnC, stabilizing its open conformation, and thus facilitating the binding of cTnI to cNTnC.[36,37] The overall conformation of cNTnC is very similar in all of these structures. They include the NMR structure of cNTnC in complex with a bepridil molecule and the $cTnI_{147–163}$ switch peptide (PDB ID: 1LX),[34] the NMR structure of cNTnC in complex with a W7 molecule (PDB ID: 2KFX)[35] and with both a W7 molecule and the $cTnI_{147–163}$ switch peptide (PDB ID: 2KRD),[38] the NMR structure of cNTnC in complex with the $cTnI_{147–163}$ switch peptide and the analog of levosimendan, 2′,4′-difluorobiphenyl-4-yloxy acetic acid (PDB ID: 2L1R),[36] and the crystal structure of cNTnC in complex with trifluoperazine (PDB ID: 1WRK) (Takeda, S., Igarashi, T., Oishi, Y., and Mori, H., unpublished data). Using the best representative chain from each NMR ensemble and the single chain from 1WRK model, the superimposition of all the aforementioned structures yields a C^{α} r.m.s.d. of 2.3 Å, indicating their similar overall conformation.

The presence of Ca^{2+} sensitizers and cTnI peptide in the hydrophobic pocket as well as Ca^{2+} binding to loop 2 induces the overall conformation of cNTnC into its open state. Without these drugs, both the apo and Ca^{2+}-bound states of cNTnC remain in the "closed" state. The open conformation of cNTnC is characterized by helices B and C linked by a short linker moving away from helices A and D, resulting in the exposure of larger core hydrophobic surface area. The structure presented here resembles the open conformation. This is most likely due to the Cd^{2+} binding to loop 2 and the presence of DXC in the hydrophobic core, which is the prerequisite for the open conformation in the other structures.

Discussions on the unique Cd^{2+} coordination in EF 1

The EF 1 of the mammalian cNTnC was shown to be incapable of Ca^{2+} binding over the range of physiological cytosolic Ca^{2+} concentrations (100–2000 nM). This explains the different thermodynamic and kinetic responses to Ca^{2+} between cTnC and sTnC.[11] Therefore, finding a Cd^{2+} coordinated by residues from the defunct EF 1 in canonical ion coordination geometry is unexpected. In some respects, the Cd^{2+} binding in EF 1 resembles the metal ion coordination by versatile noncanonical EF-hands. As previously stated, the composition and length of their ion binding loops can vary significantly from the classical sequence, yet the pentagonal bipyramid ion ligand coordination geometry can be maintained.[15,16] This is made possible in part by the conserved "scaffold" in the C-terminal part of the binding loops. The structure presented here indicates that such a scaffold is also conserved in EF 1 of cNTnC.

Without the dramatic conformational rearrangement by helix A, the EF 1 ion coordination is unlikely to be reproduced. A simple extension of helix A at the C-terminus while helices N and A maintain contacts with helix D in the usual cNTnC conformation will result in the Gly30 O ligand pointing perpendicularly away from the bound ion. It is the perpendicular "swing" of helix A around the Leu29 hinge that brings the X ligand into coordinating position. Therefore, the structure presented here does not necessarily imply that Ca^{2+} binding can occur at loop 1 in mammalian cNTnC. However, the conserved and structurally intact C-terminal part of the EF-hand motif alone is shown to provide six out of seven required ligands at Y, Z, −Y, −X, and −Z positions for canonical ion coordination (Fig. 3c). Such a coordinating scaffold probably played a role in stabilizing the considerable conformational change by cNTnC required for Cd^{2+} coordination in canonical geometry.

It is an interesting conundrum that the N-terminal region of loop 1 within the cNTnC domain in ectothermic species of vertebrates, particularly those adapted to survive at colder temperatures, has significantly different sequences. In trout cNTnC, residues Ile28, Gln29, and Asp30 replace Val28, Leu29, and Gly30 residues in human cNTnC (Fig. 1b). Moreover, they were found to be responsible for the comparatively higher Ca^{2+} affinity of trout cTnC compared to human cTnC.[10] This in turn translates to higher Ca^{2+} sensitivity of trout cardiac myocytes, which allows for normal trout cardiac function at its significantly lower physiological temperatures. These observations indicate unique but not well-understood properties conferred by these residues toward loop 1 of cNTnC, which perhaps may involve differential interaction with Ca^{2+}.

Previous NMR titration experiments suggested that Ca^{2+} binding can occur at EF 1 of trout cTnC in solution,[39] albeit with a relatively low affinity. The structure presented here demonstrates that the intact C-terminus of loop 1 is capable of providing most of the required ion coordination; thus, such binding may be possible with a favorable conformational change at the N-terminal part of the loop involving residues Ile28, Gln29, and Asp30. It is probably more than coincidence that the corresponding three residues (Val28, Leu29, and Gly30) in this human cNTnC structure are involved in the most significant disorder-to-order transition. Instead of the backbone carbonyl oxygen, perhaps the Asp30 side-chain carboxylate oxygen could provide the necessary coordination corresponding to the ligand at the X position. Aspartic acid is the most favored residue for the X position in the ion binding loop of the EF-hand motif in general.[16] If not a direct interaction, Asp30 may still be able to stabilize the Ca^{2+} binding via a water molecule or by forming a network of loop-stabilizing hydrogen bonding interactions. In summary, the crystal structure presented here provides a snapshot of an unusual conformation of cNTnC that formed in the presence of Cd^{2+} and DXC. The canonical coordination of Cd^{2+} demonstrates the preservation of functional elements in the C-terminal part of the vestigial loop that act as an important ion coordinating scaffold in various EF-hand motifs.

Materials and Methods

Cloning and mutagenesis

The full-length wild-type human cTnC was cloned into the pET21a expression plasmid (Novagen), which was used to produce the cNTnC construct that contains residues 1–89. Lys90 was converted to a termination codon by site-directed mutagenesis using the QuikChange kit (Stratagene) with the 39-base forward primer 5′-TGTATGAAAGATGACAGCTAAGGAAAATCTGAAGAGGAG-3′ and the reversed primer 5′-CTCCTCTTCAGATTTTCCTTAGCTGTCATCTTTCATACA-3′. DNA

sequencing (Macrogen) confirmed the cTnC sequence reported in the Swiss-Prot database (accession number P63316). The plasmid pET21a-cNTnC was transformed into BL21(DE3) *Escherichia coli* cells. The expressed protein (cNTnC) is 89 residues in length and has a calculated molecular mass of 10,062 Da and a theoretical isoelectric point of 4.0.

Protein over-expression and purification

Se-Met-incorporated protein was prepared by growing an overnight culture of BL21(DE3) transformed with the plasmid pET21a-cNTnC in M9 minimal medium supplemented with 100 μg/mL ampicillin. Five hundred microliters of the overnight culture was used to inoculate 100 mL of M9 minimal medium (100 μg/mL ampicillin), and 20 mL of that overnight M9 culture was used to inoculate 1 L of M9 minimal media (100 μg/mL ampicillin) that was grown for 5–6 h at 37 °C until the A_{600} reached 0.6. Each liter of culture was then supplemented with the following combination of amino acids: 100 mg each of lysine, phenylalanine, and threonine; 50 mg each of isoleucine, leucine, and valine; and 60 mg of L-selenomethionine. After 15 min, each liter of cell culture was induced with IPTG at a final concentration of 1 mM and grown for an additional 6 h at 37 °C. Cell pellets were then collected by centrifugation and resuspended with resuspension buffer [50 mM Tris–HCl (pH 7.5), 25% sucrose, 0.5 mM PMSF, and 2 mM $MgCl_2$] and ethylenediaminetetraacetic-acid-free 1× protease inhibitor cocktail (Roche). Cells were completely lysed by sonicating three times with a 5-s interval at 30% amplitude using a Model 500 Dismembrator (Fisher Scientific) and using an Avestin Emulsiflex-3C cell homogenizer. The supernatant was separated from the lysate by centrifugation at 2900*g* for 30 min. Final concentrations of 1 mM $MgCl_2$, 5 mM $CaCl_2$, 50 mM NaCl, and 1 mM DTT were added to the supernatant immediately after the centrifugation, and the supernatant was then applied to a phenyl Sepharose 6 fast flow column (5-mL column volume; GE Health Care) equilibrated with a buffer consisting of 50 mM Tris–HCl (pH 7.5), 1 mM $MgCl_2$, 5 mM $CaCl_2$, 50 mM NaCl, and 1 mM DTT. The purification of cNTnC using the phenyl Sepharose hydrophobic matrix was carried out as described by Li *et al.*[40] The elution fractions containing cNTnC were concentrated using an Amicon ultracentrifuge filter device (Millipore) with a 3-kDa molecular mass cutoff. The protein was further purified by a Sepharacryl S-100 HiPrep 26/60 size-exclusion chromatography column on an ÄKTA Prime system (Pharmacia Biotech) that was run at 1 mL/min and equilibrated with 50 mM Tris–HCl (pH 7.5), 0.2 mM $CaCl_2$, and 1 mM DTT. The fractions containing pure cNTnC were analyzed by 15% SDS-PAGE, combined, and concentrated to 10 mg/mL using an Amicon ultracentrifuge filter device (Millipore) with a 3-kDa cutoff and quantified by a NanoDrop Spectrophotometer ND-1000.

Mass spectrometry analysis

To confirm the full incorporation of selenium atoms into the cNTnC protein, we performed matrix-assisted laser desorption/ionization mass spectrometry on a MALDI-LR time-of-flight spectrometer (Waters Corp., Manchester, UK) in positive ion mode, using a matrix of sinapic acid saturated in 50% acetonitrile. The instrument was operated in linear mode with a pulse voltage of 1400 V, a source voltage of 15,000 V, a multichannel plate detector potential difference of 1850 V, and a TLF delay of 500 ns. Samples were desorbed with a nitrogen laser ($l = 337$ nm), and the ion signals detected from 50 laser shots with sample times of 5 ns were summed for each mass spectrum archived. Mass spectra were recorded over an m/z range of 2000–20,000. The proteins: myoglobin, cytochrome C, and adrenocorticotropic hormone fragment 18–39 (Sigma Chemical Co., St. Louis, MO, USA) were used as calibration standards.

Crystallization

The crystals used for SAD data collection were grown by the sitting-drop vapor diffusion method. The crystallization drops were prepared by mixing 1 μL of purified protein (10 mg/mL) with 1 μL of reservoir solution and 1 μL of 50 mM DXC and then equilibrating against 1 mL of reservoir solution. The optimized crystallization reservoir condition contained 50 mM $CdSO_4$, 900 mM sodium acetate, and 100 mM Tris–HCl (pH 8.0). The long plate-shaped crystals were grown at room temperature (293 K), and optimized crystals appeared after 3 days. Prior to data collection, crystals were transferred to a cryoprotectant solution, which consisted of the same components as the reservoir solution but with 30% of the water replaced with glycerol. Crystals were incubated in the cryoprotectant solution for approximately 10 min before they were flash cooled in liquid nitrogen.

Data collection

Diffraction data from the Se-Met-incorporated wild-type cNTnC crystals were performed at Beamline 081D-1 of the Canadian Light Source, Canadian Macromolecular Crystallography Facility, University of Saskatchewan at Saskatoon using the Mar 225 CCD X-ray detector. Se-Met data set 1 (used for heavy-atom search) was collected with a crystal-to-detector distance of 180 mm and a 1° oscillation. A total of 180 images were collected. Reflections were detectable up to 2.1 Å resolution. Se-Met data set 2 (used for structural refinement) was collected with a crystal-to-detector distance of 180 mm and 1° of oscillations. A total of 150 images were collected. The reflections were detectable to 2.2 Å.

Phasing, structure determination, and refinement

Se-Met data set 1 collected at a wavelength $\lambda = 0.98086$ was used for phase calculation by the SAD method. Diffraction images were processed with HKL3000.[41–43] The merging of data sets and corrections for radiation-induced effects were performed using a novel hierarchical procedure.[18,44] Heavy-atom position search was performed at 2.8 Å with SHELXD.[45] The map generated by SHELXE had clearly interpretable electron density and

was subsequently used for the initial model building with ARP/wARP.[44,46] The refinement of heavy-atom positions and the further phasing were performed with MLPHARE,[47] which resulted in 28 refined heavy-atom positions. This phase information was used in the model building and refinement as an additional restraint. Intensities from Se-Met data set 2 collected at wavelength $\lambda = 0.98066$ were used for structure refinement with the program REFMAC5.[48] Subsequent manual model building by visual inspection of the electron density map was carried out using Coot.[49] The final models were obtained by running restrained refinement with TLS (*T*ranslation–*L*ibration–*S*crew Rotation) restraints obtained from the TLS motion determination server.[50] The complete data collection and refinement statistics are in Table 1.

Structural analysis

The secondary structural analysis was performed with the programs DSSP[51] and PROMOTIF.[49] The programs Coot[52] and SUPERPOSE[53] were used to overlap coordinates for structural comparison. The stereochemistry of the structure was analyzed with the program PROCHECK.[54] *B*-factor analysis was performed by the program BAVERAGE within the CCP4 suite of programs.[55]

Figure preparation

Figures were prepared using PyMOL.[56] The alignment figure was prepared using the program ClustalW.[57] The chemical structure of deoxycholate was drawn by GCChemPaint.[58]

Accession numbers

Coordinates and structure factors have been deposited in the Research Collaboratory for Structural Bioinformatics PDB with accession number 3RV5.

Acknowledgements

This work was supported by a Grant-in-Aid from the Heart and Stroke Foundation of British Columbia and Yukon (G.F.T./M.P.) and operating grants from the Canadian Institutes of Health Research and the Natural Science and Engineering Research Council of Canada awarded to M.P. M.P. is a scholar of the Michael Smith Foundation for Health Research, and G.F.T. is a Canada Research Chair. We thank the staff at the macromolecular Beamline 081D-1, Canadian Light Source, Saskatoon, Canada, for their technical assistance with data collection. The Canadian Light Source is supported by Natural Science and Engineering Research Council, National Research Council, Canadian Institutes of Health Research, and the University of Saskatchewan.

Supplementary Data

Supplementary data to this article can be found online at doi:10.1016/j.jmb.2011.08.049

References

1. Farah, C. S. & Reinach, F. C. (1995). The troponin complex and regulation of muscle contraction. *FASEB J.* **9**, 755–767.
2. Gordon, A. M., Homsher, E. & Regnier, M. (2000). Regulation of contraction in striated muscle. *Physiol. Rev.* **80**, 853–924.
3. Kretsinger, R. H. & Nockolds, C. E. (1973). Carp muscle calcium-binding protein. II. Structure determination and general description. *J. Biol. Chem.* **248**, 3313–3326.
4. Strynadka, N. C. & James, M. N. (1989). Crystal structures of the helix–loop–helix calcium-binding proteins. *Annu. Rev. Biochem.* **58**, 951–998.
5. van Eerd, J. P. & Takahashi, K. (1975). The amino acid sequence of bovine cardiac tamponin-C. Comparison with rabbit skeletal troponin-C. *Biochem. Biophys. Res. Commun.* **64**, 122–127.
6. Li, M. X., Gagne, S. M., Spyracopoulos, L., Kloks, C. P., Audette, G., Chandra, M. *et al.* (1997). NMR studies of Ca^{2+} binding to the regulatory domains of cardiac and E41A skeletal muscle troponin C reveal the importance of site I to energetics of the induced structural changes. *Biochemistry*, **36**, 12519–12525.
7. Teleman, O., Drakenberg, T., Forsen, S. & Thulin, E. (1983). Calcium and cadmium binding to troponin C. Evidence for cooperativity. *Eur. J. Biochem.* **134**, 453–457.
8. Holroyde, M. J., Robertson, S. P., Johnson, J. D., Solaro, R. J. & Potter, J. D. (1980). The calcium and magnesium binding sites on cardiac troponin and their role in the regulation of myofibrillar adenosine triphosphatase. *J. Biol. Chem.* **255**, 11688–11693.
9. Spyracopoulos, L., Gagne, S. M., Li, M. X. & Sykes, B. D. (1998). Dynamics and thermodynamics of the regulatory domain of human cardiac troponin C in the apo- and calcium-saturated states. *Biochemistry*, **37**, 18032–18044.
10. Gillis, T. E., Liang, B., Chung, F. & Tibbits, G. F. (2005). Increasing mammalian cardiomyocyte contractility with residues identified in trout troponin C. *Physiol. Genomics*, **22**, 1–7.
11. Gillis, T. E., Marshall, C. R. & Tibbits, G. F. (2007). Functional and evolutionary relationships of troponin C. *Physiol. Genomics*, **32**, 16–27.
12. Hoffmann, B., Schmidt-Traub, H., Perrot, A., Osterziel, K. J. & Gessner, R. (2001). First mutation in cardiac troponin C, L29Q, in a patient with hypertrophic cardiomyopathy. *Hum. Mutat.* **17**, 524.
13. Putkey, J. A., Dotson, D. G. & Mouawad, P. (1993). Formation of inter- and intramolecular disulfide bonds can activate cardiac troponin C. *J. Biol. Chem.* **268**, 6827–6830.
14. Li, Y., Love, M. L., Putkey, J. A. & Cohen, C. (2000). Bepridil opens the regulatory N-terminal lobe of cardiac troponin C. *Proc. Natl Acad. Sci. USA*, **97**, 5140–6830.

15. Grabarek, Z. (2006). Structural basis for diversity of the EF-hand calcium-binding proteins. *J. Mol. Biol.* **359**, 509–525.
16. Gifford, J. L., Walsh, M. P. & Vogel, H. J. (2007). Structures and metal-ion-binding properties of the $Ca2^{+}$-binding helix–loop–helix EF-hand motifs. *Biochem. J.* **405**, 199–221.
17. Borek, D., Ginell, S. L., Cymborowski, M., Minor, W. & Otwinowski, Z. (2007). The many faces of radiation-induced changes. *J. Synchrotron Radiat.* **14**, 24–33.
18. Borek, D., Cymborowski, M., Machius, M., Minor, W. & Otwinowski, Z. (2010). Diffraction data analysis in the presence of radiation damage. *Acta Crystallogr., Sect. D: Biol. Crystallogr.* **66**, *426–436.*
19. Rao, S. T., Satyshur, K. A., Greaser, M. L. & Sundaralingam, M. (1996). X-ray structures of Mn, Cd and Tb metal complexes of troponin C. *Acta Crystallogr., Sect. D: Biol. Crystallogr.* **52**, *916–922.*
20. Forsen, S., Thulin, E. & Lilja, H. (1979). ^{113}Cd NMR in the study of calcium binding proteins: troponin C. *FEBS Lett.* **104**, 123–126.
21. Dokmanic, I., Sikic, M. & Tomic, S. (2008). Metals in proteins: correlation between the metal-ion type, coordination number and the amino-acid residues involved in the coordination. *Acta Crystallogr. Sect. D: Biol. Crystallogr.* **64**, *257–263.*
22. Takeda, S., Yamashita, A., Maeda, K. & Maeda, Y. (2003). Structure of the core domain of human cardiac troponin in the Ca(2+)-saturated form. *Nature*, **424**, 35–41.
23. Akke, M., Forsen, S. & Chazin, W. J. (1995). Solution structure of (Cd^{2+})1-calbindin D9k reveals details of the stepwise structural changes along the Apo$\rightarrow(Ca^{2+})$II1$\rightarrow(Ca^{2+})$I,II2 binding pathway. *J. Mol. Biol.* **252**, 102–121.
24. Andersen, O. (1984). Chelation of cadmium. *Environ. Health Perspect.* **54**, 249–266.
25. Nagae, M., Nozawa, A., Koizumi, N., Sano, H., Hashimoto, H., Sato, M. & Shimizu, T. (2003). The crystal structure of the novel calcium-binding protein AtCBL2 from *Arabidopsis thaliana*. *J. Biol. Chem.* **278**, 42240–42246.
26. Tanaka, T., Ames, J. B., Harvey, T. S., Stryer, L. & Ikura, M. (1995). Sequestration of the membrane-targeting myristoyl group of recoverin in the calcium-free state. *Nature*, **376**, 444–447.
27. Ames, J. B., Ishima, R., Tanaka, T., Gordon, J. I., Stryer, L. & Ikura, M. (1997). Molecular mechanics of calcium–myristoyl switches. *Nature*, **389**, 198–202.
28. Hofmann, A. F. (1999). The continuing importance of bile acids in liver and intestinal disease. *Arch. Intern. Med.* **159**, 2647–2658.
29. Neugebauer, J. M. (1990). Detergents: an overview. *Methods Enzymol.* **182**, 239–253.
30. Wang, X., Li, M. X., Spyracopoulos, L., Beier, N., Chandra, M., Solaro, R. J. & Sykes, B. D. (2001). Structure of the C-domain of human cardiac troponin C in complex with the Ca^{2+} sensitizing drug EMD 57033. *J. Biol. Chem.* **276**, 25456–25466.
31. Robertson, I. M., Baryshnikova, O. K., Li, M. X. & Sykes, B. D. (2008). Defining the binding site of levosimendan and its analogues in a regulatory cardiac troponin C–troponin I complex. *Biochemistry*, **47**, 7485–7495.
32. Endoh, M. (2007). Could Ca^{2+} sensitizers rescue patients from chronic congestive heart failure? *Br. J. Pharmacol.* **150**, 826–828.
33. Kass, D. A. & Solaro, R. J. (2006). Mechanisms and use of calcium-sensitizing agents in the failing heart. *Circulation*, **113**, 305–315.
34. Wang, X., Li, M. X. & Sykes, B. D. (2002). Structure of the regulatory N-domain of human cardiac troponin C in complex with human cardiac troponin I147-163 and bepridil. *J. Biol. Chem.* **277**, 31124–31133.
35. Hoffman, R. M. & Sykes, B. D. (2009). Structure of the inhibitor W7 bound to the regulatory domain of cardiac troponin C. *Biochemistry*, **48**, 5541–5552.
36. Robertson, I. M., Sun, Y. B., Li, M. X. & Sykes, B. D. (2010). A structural and functional perspective into the mechanism of Ca(2+)-sensitizers that target the cardiac troponin complex. *J. Mol. Cell. Cardiol.* **49**, 1031–1041.
37. Li, M. X., Robertson, I. M. & Sykes, B. D. (2008). Interaction of cardiac troponin with cardiotonic drugs: a structural perspective. *Biochem. Biophys. Res. Commun.* **369**, 88–99.
38. Oleszczuk, M., Robertson, I. M., Li, M. X. & Sykes, B. D. (2010). Solution structure of the regulatory domain of human cardiac troponin C in complex with the switch region of cardiac troponin I and W7: the basis of W7 as an inhibitor of cardiac muscle contraction. *J. Mol. Cell. Cardiol.* **48**, 925–933.
39. Gillis, T. E., Blumenschein, T. M., Sykes, B. D. & Tibbits, G. F. (2003). Effect of temperature and the F27W mutation on the Ca^{2+} activated structural transition of trout cardiac troponin C. *Biochemistry*, **42**, 6418–6426.
40. Li, M. X., Chandra, M., Pearlstone, J. R., Racher, K. I., Trigo-Gonzalez, G., Borgford, T. *et al.* (1994). Properties of isolated recombinant N and C domains of chicken troponin C. *Biochemistry*, **33**, 917–925.
41. Minor, W., Cymborowski, M., Otwinowski, Z. & Chruszcz, M. (2006). HKL-3000: the integration of data reduction and structure solution—from diffraction images to an initial model in minutes. *Acta Crystallogr., Sect. D: Biol. Crystallogr.* **62**, *859–866.*
42. Otwinowski, Z. & Minor, W. (1997). Processing of X-ray diffraction data collected in oscillation mode. In *Methods Enzymol.* (Carter, C. W. & Sweet, R. M., eds), Vol. 276, pp. 307–326, Academic Press, New York, NY.
43. Otwinowski, Z. & Minor, W. (2000). Denzo and Scalepack. In *International Tables for Crystallography* (Rossman, M. G., ed.), Vol. F, pp. 226–235. Kluwer Academic Publishers, Dordrecht, Netherlands.
44. Tikhonov, A. N. & Arsenin, V. Y. (1977). *Solutions of Ill-Posed Problems.* Winston and Sons distributed by Wiley and Sons, New York, NY.
45. Sheldrick, G. M. (2008). A short history of SHELX. *Acta Crystallogr., Sect. A: Found. Crystallogr.* **64**, 112–122.
46. Perrakis, A., Sixma, T. K., Wilson, K. S. & Lamzin, V. S. (1997). wARP: improvement and extension of crystallographic phases by weighted averaging of multiple-refined dummy atomic models. *Acta Crystallogr., Sect. D: Biol. Crystallogr.* **53**, *448–455.*
47. Otwinowski, Z., (1991). Maximum likelihood refinement of heavy atom parameters. CCP4 Study Weekend Proceedings Isomorphous Replacement and Anomalous Scattering, 80–87.

48. Winn, M. D., Isupov, M. N. & Murshudov, G. N. (2001). Use of TLS parameters to model anisotropic displacements in macromolecular refinement. *Acta Crystallogr., Sect. D: Biol. Crystallogr.* **57**, *122–133.*
49. Hutchinson, E. G. & Thornton, J. M. (1996). PROMOTIF—a program to identify and analyze structural motifs in proteins. *Protein Sci.* **5**, 212–220.
50. Painter, J. & Merritt, E. A. (2006). Optimal description of a protein structure in terms of multiple groups undergoing TLS motion. *Acta Crystallogr., Sect. D: Biol. Crystallogr.* **62**, *439–450.*
51. Kabsch, W. & Sander, C. (1983). Dictionary of protein secondary structure: pattern recognition of hydrogen-bonded and geometrical features. *Biopolymers*, **22**, 2577–2637.
52. Emsley, P. & Cowtan, K. (2004). Coot: model-building tools for molecular graphics. *Acta Crystallogr., Sect. D: Biol. Crystallogr.* **60**, *2126–2132.*
53. Maiti, R., Van Domselaar, G. H., Zhang, H. & Wishart, D. S. (2004). SuperPose: a simple server for sophisticated structural superposition. *Nucleic Acids Res.* **32**, W590–W594.
54. Laskowski, R. A., MacArthur, M. W., Moss, D. S. & Thornton, J. M. (1993). PROCHECK: a program to check the stereochemical quality of protein structures. *J. Appl. Crystallogr.* **26**, 283–291.
55. Number 4, C. C. P (1994). The CCP4 suite: programs for protein crystallography. *Acta Crystallogr., Sect. D: Biol. Crystallogr.* **D50**, *760–763.*
56. DeLano, W. L. (2002). *The PyMOL Molecular Graphics System.* DeLano Scientific, San Carlos, CA.
57. Thompson, J. D., Higgins, D. G. & Gibson, T. J. (1994). Improved sensitivity of profile searches through the use of sequence weights and gap excision. *Comput. Appl. Biosci.* **10**, 19–29.
58. Brefort, J. (2001). GChemPaint 0.8.7.